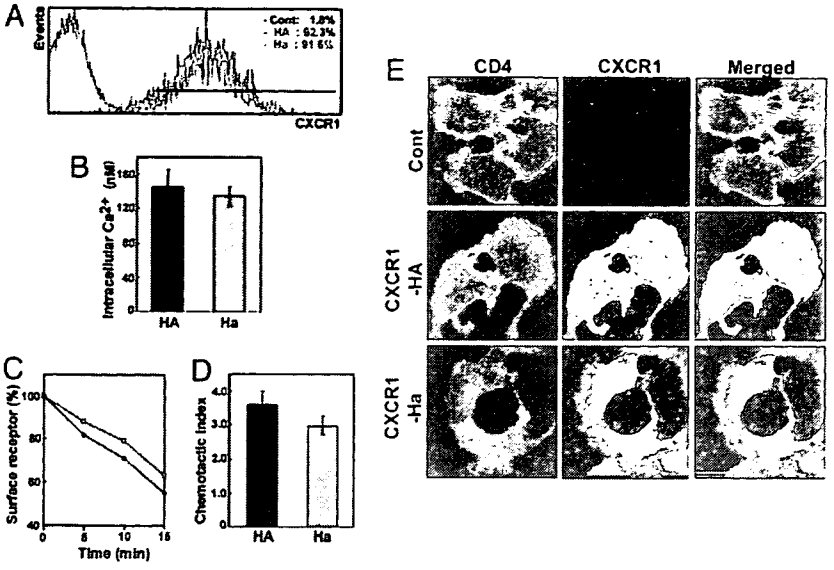

Fig. 3. CXCR1 expression and cellular responses to its cognate ligand IL-8 by using HOS cells. (*A*) Flow cytometric analysis of CXCR1 expression. (*B*) Intracellular Ca^{2+} mobilization. (*C*) Receptor internalization. (*D*) Chemotactic activity. (*E*) Confocal fluorescence microscopic images showing the subcellular distribution of CD4 (left column, green) and *CXCR1-HA* or *CXCR1-Ha* (middle column, red) on each transfected HOS cells. Overlaid green and red images show the colocalization between CD4 and CXCR1 (right column, yellow).

transduction by altering interaction with signaling and regulatory proteins (20). Moreover, extensive site-directed mutagenesis studies have failed to demonstrate significance of the methionine substitution at the *CXCR1_300* position for IL-8 binding and calcium flux (21).

Association of CXCR1 and CXCR2 SNPs with AIDS Progression. The relationship of the 21 variants of *CXCR1* and *CXCR2* to AIDS progression was evaluated by genotyping of the GRIV cohort (22), consisting of 253 asymptotic HIV-1 seropositive individuals (SP series) and 84 patients with rapid disease progression (RP series). To validate the cohort, we examined the *CCR5 delta-32* polymorphism. The results are compatible with previous studies in which *CCR5 delta-32* has been shown to restrict infection in homozygous individuals and to reduce disease progression in the heterozygous state in Caucasians (8–10, 23). We found no individuals homozygous for the *CCR5 delta-32* allele in GRIV compared with two individuals in the CTR series. The frequency of *CCR5 delta-32* was 12% in the SP series, 7% in the CTR series, and 2% in the RP series ($P = 0.0002$), confirming its association with progression.

The frequencies of the common *CXCR1–CXCR2* polymorphisms in the CTR, SP, and RP series are shown in Table 1. Significant differences in allele frequencies among the groups were found for seven SNPs ($P < 0.001$). Of particular interest, only the two sites involving nonsynonymous amino acid substitutions (*CXCR1_300* and *CXCR1_142*) and the others in strong LD with these (*CXCR1_219*, *CXCR1_200*, *CXCR2_7222390*, and *CXCR2_7222360*) showed significant frequency differences. At these six sites, the minor alleles were absent in the RP series, whereas the corresponding frequencies of these alleles in the SP and CTR series were ≈6% and ≈4%, respectively. The most extreme allele frequencies in the SP and RP series, with the CTR intermediate, is similar to those in *CCR5* and compatible with association to progression. The haplotype carrying the minor alleles at the six strongly associated sites (designated *Ha*) was absent in the RP series and has significantly higher frequencies in SP and CTRs ($P = 0.001$ for SP vs. CTR vs. RP; $P = 0.0003$ for SP vs. RP; see Table 2). To determine if these associations could be due to variants in neighboring genes in LD with a *CXCR1–CXCR2* locus, we performed SNP identification of the two flanking genes, *ARPC2* (50-kb telomeric to *CXCR1*) and *FLJ46536* (35-kb centromeric to *CXCR2*). None of the polymorphisms detected exhibited significant LD with *CXCR1* or *CXCR2* variants, demonstrating that the disease-associated haplotype does not extend to the neighboring genes.

Discussion

Our results afford strong biological and genetic evidence of a protective role of *CXCR1* variants on HIV-1 disease progression. As discussed above, the *CCR5 delta-32* variant is also known to be associated with resistance to $CD4^+$ cell depletion, but different mechanisms are likely to underlie between the involvement of CCR5 and CXCR1 in disease progression. *CCR5 delta-32* gives rise to a truncated CCR5 molecule that forms heterocomplexes with intact CCR5 in the endoplasmic reticulum, leading to reduced CCR5 cell-surface density and contributing to slower disease progression in heterozygotes (8–10). The major effect of the reduced CCR5 density appears to be modulation of virus replication cycle in early stages, particularly of reverse transcription (24).

In contrast, the inhibitory effects of variant CXCR1 on the X4-tropic HIV-1 infection are likely to be a consequence of the suppressed expression of CD4 and CXCR4. The importance of CXCR1 in disease progression may be related to the Th1-to-Th2 shift observed in the later stages of AIDS. In atopic patients, this shift has been associated with an increase of $CXCR1^+CD4^+$ cells (25). The lower expression of CD4 and CXCR4 in *CXCR1-Ha* cells demonstrated in our study could be caused by unknown CXCR1-mediated signaling that regulates expression and intracellular trafficking of CD4 and CXCR4. Coexpression of CCR5 and CXCR4 interferes with HIV-1 entry under low density of cell surface CD4 (26), and the appearance of CXCR4 tropic HIV-1 variants in later stages of infection is associated with a decline in $CD4^+$ T cell counts and adverse clinical prognosis of AIDS (25). Direct involvement of reduced CXCR1-mediated signals in HIV-1 replication is also possible (18) through palmitoylation of *CXCR1-Ha* at the cysteine introduced in the C-terminal intracellular domain. Indeed, palmitoylation of C-terminal cysteine in CCR5 is known to modify receptor trafficking and activation of intracellular signaling pathways (27). Genetic association of the *CXCR1-Ha* haplotype with chronic obstructive pulmonary disease and asthma was reported (28). It is interesting to examine functional roles of the variant CXCR1 molecule in inflammatory response.

Materials and Methods

Patients and Control Subjects. The GRIV cohort was established in 1995 in France to generate a large collection of DNAs for genetic

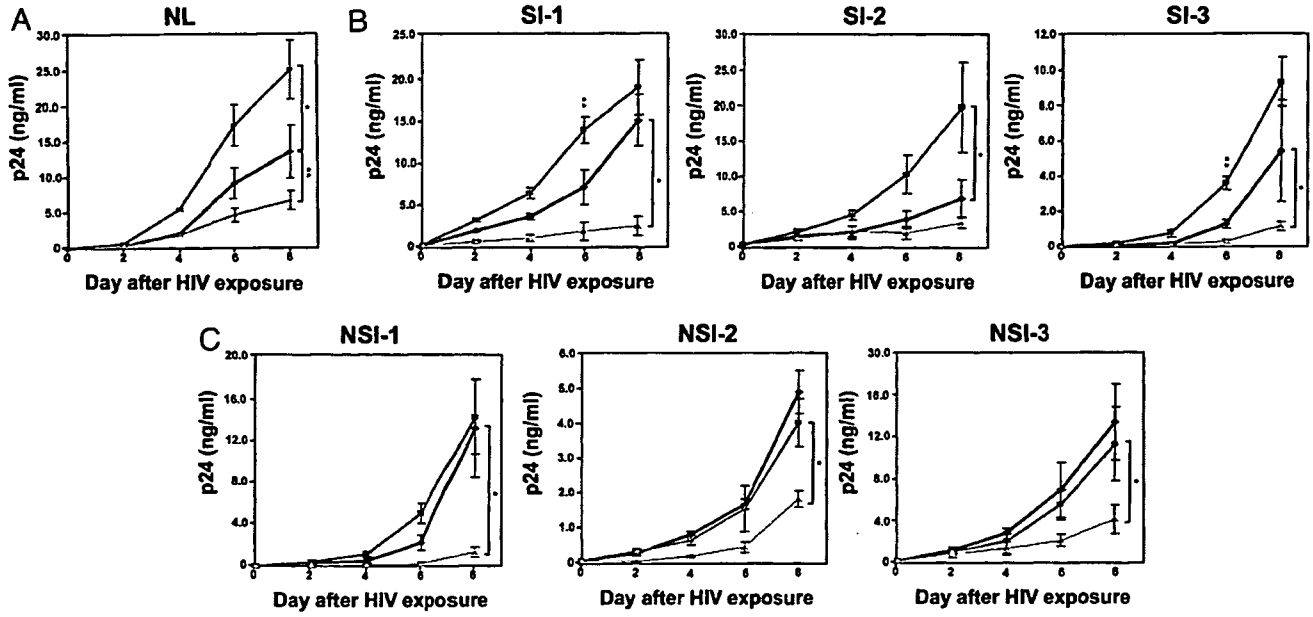

Fig. 4. The efficiency of X4-tropic HIV infection in HOS cells transfectants by using HIV-1_{NL4-3} strain (*A*), S.I. clinical isolates (*B*), and N.S.I. clinical isolates (*C*). S.I. represents an isolate with CXCR4 predominance, and N.S.I. represents and isolate with CCR5 predominance. Red, blue, and black lines show the means from three three-replicate assays for *CXCR1-Ha* (red lines), *CXCR1-HA* (blue lines) and control cells transfected with empty vector (black lines). Vertical bars indicate the range of the results obtained for each set of measurements. The amount of p24 protein in culture medium is indicated as ng/ml. Differences between *CXCR1-Ha* and *CXCR1-HA* for day 8 are significant in all instances as evaluated by a *t* test: NL, $P = 0.002$; S.I.-1, $P = 0.001$; S.I.-2, $P = 0.01$; S.I.3, $P = 0.008$; N.S.I.-1, $P = 0.003$; N.S.I.-2, $P = 0.006$; N.S.I.-3, $P = 0.03$.

studies on candidate polymorphisms associated with rapid and slow progression of AIDS (22). This cohort consists of two subpopulations with extreme phenotypes selected from a pool of ≈25,000 French HIV-1^+ individuals: 253 asymptomatic individuals with a $CD4^+$ cell count >500/mm^3 for 8 or more years after seroconversion (SP series) and 84 patients with rapid progression showing a drop in their $CD4^+$ cell count <300/mm^3 in <3 years after the last seronegative test (RP series). We estimated that the RP and SP series represented the 1% extremes of seropositive patients seen in the participating clinics in France (22). Members of the cohort were diagnosed with a seropositive test before 1996, and all are of French Caucasian origin. All patients enrolled in the study gave informed consent. The data on 471 CTR subjects of the same ethnic origin with unknown HIV status were obtained as part of the Epidemiological Study on the Genetics and Environment of Asthma (EGEA) study of asthma (29). DNA was obtained from fresh peripheral blood mononuclear cells or from EBV-transformed cell lines.

SNP Identification and Genotyping. Oligonucleotide primers were designed to amplify the exon-containing DNA fragments and the promoters by PCR [see supporting information (SI) Table 3]. Nucleotide sequencing was performed by the dye terminator method with an ABI PRISM 3700 DNA analyzer (Applied Biosystems, Foster City, CA). Results were aligned to NT_005403.10 and analyzed for SNP discovery and genotyping with the software Genalys (30). Genotypes of SNPs that showed statistical significance were reconfirmed by Taqman technology (Applied Biosystems). Information about all of the SNPs, including those with a frequency of <1%, is also available from the Centre National de Génotypage (CNG) web site (SI Table 4).

Statistics. Differences in the allele frequencies of individual polymorphisms among the three groups and between the SP and RP groups were examined by using a Fisher's exact test on the resulting 2 × 3 or 2 × 2 tables of counts. *P* values were also adjusted by performing a randomization test in which phenotype status (RP, SP, or CTR) was reassigned to the different individuals, conserving the multilocus genotypes to preserve LD. The adjusted *P* value at a specific locus was calculated as frequency over 50,000 replicates of obtaining a result at any locus as or more extreme than that observed at the specific locus. Haplotype frequencies using all polymorphisms for each gene were estimated with an EM algorithm. Differences between haplotype frequencies were examined in an analogous way to that used for the individual polymorphisms, except that within each series, expected haplotype numbers were computed from the estimated marginal haplotype probability distribution. These numbers were rounded to the nearest integer, and *P* values were computed by using Fisher's exact test.

Cell Culture, Transfection, and Flow Cytometry. HOS/CD4.CCR5 (HOS), Jurkat, and CEM cells were maintained in DMEM or RPMI medium 1640 supplement with 10% heat-inactivated FBS, 100 units/ml penicillin, and 100 mg/ml streptomycin. The coding sequences of *CXCR1* corresponding to amino acids nos. 2–350 were amplified by PCR using specific oligonucleotide primers (SI Table 3) and were inserted into the EcoRI site of the pRc/CMV-tag vector. The constructs were checked by nucleotide sequencing for the ORF, orientation and *Taq* errors. Transfections were performed by using LipofectAMINE 2000 (Invitrogen, Carlsbad, CA). Geneticin (800 μg/ml)-resistant cells were cloned by fluorescence-activated cell sorter system EPICS ELITE ESP (Beckman Coulter, Hialeah, FL). For flow cytometric analysis, transfected HOS cells were incubated with anti-CXCR1, anti-CD4, anti-CXCR4, or anti-CCR5 antibody (DAKO, Carpinteria, CA) in PBS (pH 7.3) with 0.1% FBS for 60 min at 4°C. The cells were then washed, and analyzed for cell-surface expression of the receptor by using a flow cytometry EPICS-XL (Beckman Coulter) fitted with a single 15-mW argon ion laser providing excitation at 488 nm. FITC and phycoerythrin, respectively, were monitored through 525- and 575-nm bandpass filters.

For the expression analysis of CD4 in peripheral blood leuko-

cytes, blood samples were collected in Na_2EDTA tubes and stained within 6 h. Fifty microliters of blood was gently mixed with 1 ml of red blood cell lysis buffer and incubated at room temperature for 30 min. The sample was then centrifuged at 340 × *g* for 5 min at 4°C. The leukocyte pellet was washed twice with cold PBS. The supernatant was discarded, leaving 10 μl of fluid to resuspend the cell pellet. Five microliters of anti-CXCR1 and anti-CD4 antibodies were added to the cell suspension, and the staining reaction was incubated on ice for 1 h. After centrifugation at 340 × *g* for 5 min at 4°C, the cells were washed twice with cold PBS and analyzed by a FACS machine.

RT-PCR, Western Blot Analysis, and Immunohistochemical Analysis. RT-PCR was performed according to the standard procedures with 35 cycles by using specific primers for human *CXCR1*, *CD4*, *CXCR4*, and *CCR5*. At the same time, constitutively expressed GAPDH mRNA was amplified as an internal standard. For Western blot analysis, HOS cells (5×10^5) were suspended in loading buffer [50 mM Tris (pH 7)/3% SDS/10% glycerol/5% 2-ME] and applied on polyacrylamide gel. After electrophoresis, proteins were electrotransferred to nitrocellulose membrane (Amersham Pharmacia Biotech, Piscataway, NJ), and blotted by using each primary antibody [goat anti-CD4 (C-18; Santa Cruz Biotechnology, Santa Cruz, CA), goat anti-CCR5 (CKR5; C-20; Santa Cruz Biotechnology), rabbit anti-CXCR4 (fusin; H-118; Santa Cruz Biotechnology), or mouse anti-actin antibody (C-4; Chemicon, Temecula, CA) in accordance to the manufacturer's instructions. Blots were developed with ECL reagent (Amersham Pharmacia Biotech). For immunohistochemical analysis, HOS cells were fixed with 2% paraformaldehyde in PBS, rinsed with PBS, and then treated with 0.2% Triton X-100 in PBS. The cells were incubated with fluorescence-labeled anti-CD4 and anti-CXCR1 antibodies. Images were collected with a confocal microscope (Olympus, Melville, NY).

HIV-1 Infectivity Assay. Clinical HIV-1 isolates were obtained from the plasma derived from HIV-1-infected individuals by using MAGIC-5 cells. The ability to induce syncytia formation of clinical isolates was examined in MT-2 cells. All transfected HOS cells (5×10^3) were exposed to 100 blue-cell-forming units (measured by MAGIC-5 cells) of HIV-1_{NL4-3} or an HIV-1 clinical isolate in 500 μl of medium for 2 h. Infected cells were washed twice with PBS and cultured in 1 ml of medium. On days 2, 4, 6, and 8 of infection, 10-μl aliquots of culture supernatants were filtered and stocked for measurements of p24 antigen concentration. The concentration of p24 in each supernatant was determined by chemiluminescence enzyme immuno-assay (CLEIA) kit (Fuji-Rebio, Tokyo, Japan). Assays were performed in triplicate.

Intracellular [Ca^{2+}] Measurement and Chemotaxis Assays. For the calcium influx study, HOS cells (10^6) were washed with Tyrode's salt solution (TSS) (Sigma, St. Louis, MO) and incubated with 4 μM Fluo-3 acetoxymethyl ester in DMSO containing 20% Pluronic F-127 (Molecular Probes, Eugene, OR) at room temperature in the dark for 1 h. After washing with the same buffer, the cells were suspended in TSS containing 0.1% BSA buffer and transferred to 96 black well plates (Nunclon) for reading. Recombinant human IL-8 (final concentration, 100 nM) was added to each sample for stimulation, and fluorescence was monitored for 3 min with the microfluorescence recorder Fluoroskan Ascent system (Labsystems, Chicago, IL). Intracellular calcium concentrations were computed as described in the manufacturer's instructions. Background stabilization and probe levels were determined for each sample. Chemotaxis of all transfected Jurkat cells in response to 10-nM recombinant IL-8 was evaluated in triplicate by using a 96-well microchemotaxis chamber (Neuro Probe, Gaithersburg, MD) and a 3-μm polycarbonate membrane. RPMI medium 1640 supplemented with 10% FBS, 0.1% BSA, and 10-mM Hepes was used for the assay. Migrated cells in the lower chamber were counted by a flow cytometer EPICS-XL (Beckman Coulter).

We thank all patients and medical staff who were concerned with the establishment of the GRIV cohort and the Epidemiological Study on the Genetics and Environment of Asthma (EGEA) cooperative group, who allowed us access to data on the EGEA study, which is partly supported by an Institut National de la Santé et de la Recherche Médicale/Merck Sharp & Dohme convention. We also thank M. Alizon for his help in the construction of the vectors for transfection experiments and M. Matsuoka for valuable suggestions. V.P., P.A., and T.S. are research members of the Core University Program, which is supported by the Japan Society for the Promotion of Science. The Centre National de Génotypage is supported by the Ministere de la Recherche et des Nouvelles Technologies. The work was supported in part by Core Research for Evolutional Science and Technology, Solution Oriented Research for Science and Technology, the Japan Science and Technology Agency, the Japan Science Foundation, Agence Nationale de Recherche sur le SIDA, and the AIDS–Cancer Vaccine Development Foundation.

1. McCune JM (2001) *Nature* 410:974–979.
2. Taylor JM, Tan SJ, Detels R, Giorgi JV (1991) *AIDS* 5:159–167.
3. Haynes BF, Pantaleo G, Fauci AS (1996) *Science* 271:324–328.
4. Cocchi F, DeVico AL, Garzino-Demo A, Arya SK, Gallo RC, Lusso P (1995) *Science* 270:1811–1815.
5. Deng H, Liu R, Ellmeier W, Choe S, Unutmaz D, Burkhart M, Di Marzio P, Marmon S, Sutton RE, Hill CM, *et al.* (1996) *Nature* 381:661–666.
6. Dragic T, Litwin V, Allaway GP, Martin SR, Huang Y, Nagashima KA, Cayanan C, Maddon PJ, Koup RA, Moore JP, Paxton WA (1996) *Nature* 381:667–673.
7. Feng Y, Broder CC, Kennedy PE, Berger EA (1996) *Science* 272:872–877.
8. Samson M, Libert F, Doranz BJ, Rucker J, Liesnard C, Farber CM, Saragosti S, Lapoumeroulie C, Cognaux J, Forceille C, *et al.* (1996) *Nature* 382:722–725.
9. Dean M, Carrington M, Winkler C, Huttley GA, Smith MW, Allikmets R, Goedert JJ, Buchbinder SP, Vittinghoff E, Gomperts E, *et al.* (1996) *Science* 273:1856–1862.
10. Liu R, Paxton WA, Choe S, Ceradini D, Martin SR, Horuk R, MacDonald ME, Stuhlmann H, Koup RA, Landau NR (1996) *Cell* 86:367–377.
11. Baggiolini M, Dewald B, Moser B (1997) *Annu Rev Immunol* 15:675–705.
12. Schroder JM, Mrowietz U, Morita E, Christophers E (1987) *J Immunol* 139:3474–3483.
13. Yoshimura T, Matsushima K, Tanaka S, Robinson EA, Appella E, Oppenheim JJ, Leonard EJ (1987) *Proc Natl Acad Sci USA* 84:9233–9237.
14. Larsen CG, Anderson AO, Appella E, Oppenheim JJ, Matsushima K (1989) *Science* 243:1464–1466.
15. Matsumoto T, Miike T, Nelson RP, Trudeau WL, Lockey RF, Yodoi J (1993) *Clin Exp Immunol* 93:149–151.
16. Meddows-Taylor S, Martin DJ, Tiemessen CT (1999) *Clin Diagn Lab Immunol* 6:345–351.
17. Meddows-Taylor S, Martin DJ, Tiemessen CT (1998) *J Infect Dis* 177:921–930.
18. Lane BR, Lore K, Bock PJ, Andersson J, Coffey MJ, Strieter RM, Markovitz DM (2001) *J Virol* 75:8195–8202.
19. Richardson RM, Tokunaga K, Marjoram R, Sata T, Snyderman R (2003) *J Biol Chem* 278:15867–15873.
20. Qanbar R, Bouvier M (2003) *Pharmacol Ther* 97:1–33.
21. Leong SR, Kabakoff RC, Hebert CA (1994) *J Biol Chem* 269:19343–19348.
22. Hendel H, Cho YY, Gauthier N, Rappaport J, Schachter F, Zagury JF (1996) *Biomed Pharmacother* 50:480–487.
23. Rappaport J, Cho YY, Hendel H, Schwartz EJ, Schachter F, Zagury JF (1997) *Lancet* 349:922–923.
24. Lin YL, Mettling C, Portales P, Reynes J, Clot J, Corbeau P (2002) *Proc Natl Acad Sci USA* 99:15590–15595.
25. Connor RI, Sheridan KE, Ceradini D, Choe S, Landau NR (1997) *J Exp Med* 185:621–628.
26. Lee S, Lapham CK, Chen H, King L, Manischewitz J, Romantseva T, Mostowski H, Stantchev TS, Broder CC, Golding H (2000) *J Virol* 74:5016–5023.
27. Blanpain C, Wittamer V, Vanderwinden JM, Boom A, Renneboog B, Lee B, Le Poul E, El Asmar L, Govaerts C, Vassart G, *et al.* (2001) *J Biol Chem* 276:23795–23804.
28. Stemmler S, Arinir U, Klein W, Rohde G, Hoffjan S, Wirkus N, Reinitz-Rademacher K, Bufe A, Schultze-Werninghaus G, Epplen JT (2006) *Genes Immun* 6:225–230.
29. Kauffmann F, Dizier MH, Pin I, Paty E, Gormand F, Vervloet D, Bousquet J, Neukirch F, Annesi I, Oryszczyn MP, *et al.* (1997) *Am J Respir Crit Care Med* 156:S123–S129.
30. Takahashi M, Matsuda F, Margetic N, Lathrop M (2003) *J Bioinform Comput Biol* 1:253–265.

ACCOUNTS
of chemical research

Design of HIV Protease Inhibitors Targeting Protein Backbone: An Effective Strategy for Combating Drug Resistance

ARUN K. GHOSH,*,† BRUNO D. CHAPSAL,† IRENE T. WEBER,‡ AND HIROAKI MITSUYA§,⊥

†Departments of Chemistry and Medicinal Chemistry, Purdue University, West Lafayette, Indiana 47907, ‡Department of Biology, Molecular Basis of Disease Program, Georgia State University, Atlanta, Georgia 30303, §Departments of Hematology and Infectious Diseases, Kumamoto University School of Medicine, Kumamoto 860-8556, Japan, and ⊥Experimental Retrovirology Section, HIV and AIDS Malignancy Branch, National Cancer Institute, Bethesda, Maryland 20892

RECEIVED ON MAY 18, 2007

CONSPECTUS

The discovery of human immunodeficiency virus (HIV) protease inhibitors (PIs) and their utilization in highly active antiretroviral therapy (HAART) have been a major turning point in the management of HIV/acquired immune-deficiency syndrome (AIDS). However, despite the successes in disease management and the decrease of HIV/AIDS-related mortality, several drawbacks continue to hamper first-generation protease inhibitor therapies. The rapid emergence of drug resistance has become the most urgent concern because it renders current treatments ineffective and therefore compels the scientific community to continue efforts in the design of inhibitors that can efficiently combat drug resistance.

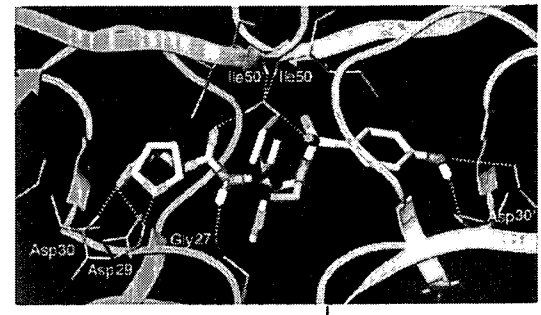

Darunavir (TMC-114)
K_i = 16 pM
IC_{90} = 4.1 nM

The present line of research focuses on the presumption that an inhibitor that can maximize interactions in the HIV-1 protease active site, particularly with the enzyme backbone atoms, will likely retain these interactions with mutant enzymes. Our structure-based design of HIV PIs specifically targeting the protein backbone has led to exceedingly potent inhibitors with superb resistance profiles.

We initially introduced new structural templates, particulary nonpeptidic conformationally constrained P_2 ligands that would efficiently mimic peptide binding in the S_2 subsite of the protease and provide enhanced bioavailability to the inhibitor. Cydic ether derived ligands appeared as privileged structural features and allowed us to obtain a series of potent PIs. Following our structure-based design approach, we developed a high-affinity 3(*R*),3a(*R*),6a(*R*)-bis-tetrahydrofuranylurethane (bis-THF) ligand that maximizes hydrogen bonding and hyrophobic interactions in the protease S_2 subsite. Combination of this ligand with a range of different isosteres led to a series of exceedingly potent inhibitors.

Darunavir, initially TMC-114, which combines the bis-THF ligand with a sulfonamide isostere, directly resulted from this line of research. This inhibitor displayed unprecedented enzyme inhibitory potency (K_i = 16 pM) and antiviral activity (IC_{90} = 4.1 nM). Most importantly, it consistently retained is potency against highly drug-resistant HIV strains. Darunavir's IC_{50} remained in the low nanomolar range against highly mutated HIV strains that displayed resistance to most available PIs.

Our detailed crystal structure analyses of darunavir-bound protease complexes clearly demonstrated extensive hydrogen bonding between the inhibitor and the protease backbone. Most strikingly, these analyses provided ample evidence of the unique contribution of the bis-THF as a P_2-ligand. With numerous hydrogen bonds, bis-THF was shown to closely and tightly bind to the backbone atoms of the S_2 subsite of the protease. Such tight interactions were consistently observed with mutant proteases and might therefore account for the unusually high resistance profile of darunavir. Optimization attempts of the backbone binding in other subsites of the enzyme, through rational modifications of the isostere or tailor made P_2 ligands, led to equally impressive inhibitors with excellent resistance profiles.

The concept of targeting the protein backbone in current structure-based drug design may offer a reliable strategy for combating drug resistance.

Published on the Web 08/28/2007 www.pubs.acs.org/acr
10.1021/ar7001232 CCC: $40.75

Introduction

Acquired immunodeficiency syndrome (AIDS), a degenerative disease of the immune system, is caused by the human immunodeficiency virus (HIV).[1,2] The current statistics for global HIV/AIDS are staggering, as an estimated 40 million people worldwide are ailing with HIV/AIDS.[3] The discovery of HIV as the etiological agent for AIDS and subsequent investigation of the molecular events critical to the HIV replication cycle led to the identification of a number of important biochemical targets for AIDS chemotherapy.[4] During viral replication, *gag* and *gag-pol* gene products are translated into precursor polyproteins. These proteins are processed by the virally encoded protease to produce structural proteins and essential viral enzymes, including protease, reverse transcriptase, and integrase.[5] Therefore, inhibition of the virally encoded HIV protease was recognized as a viable therapeutic target.[6] Since the FDA approval of the first protease inhibitor (PI) in 1995,[7] several other PIs quickly followed. The development of these PIs and their introduction into highly active antiretroviral therapy (HAART) with reverse transcriptase inhibitors marked the beginning of an important era of AIDS chemotherapy. The HAART treatment regimens arrested the progression of AIDS and significantly reduced AIDS-related deaths in the United States and other industrialized nations.[8] Despite this undeniable success, there are severe limitations of the current treatment regimens including (i) debilitating side effects and drug toxicities, (ii) higher therapeutic doses due to "peptide-like" character, and (iii) expensive synthesis and high treatment cost. Perhaps most concerning of all is the emergence of drug resistance which renders treatment ineffective in a short time. The current HAART treatment regimens are not sufficiently potent to combat multidrug-resistant HIV strains. At least 40–50% of those patients who initially achieve favorable viral suppression to undetectable levels eventually experience treatment failure.[9] Additionally, 20–40% of antiviral therapy-naive individuals infected with HIV-1 have persistent viral replication under HAART, possibly due to primary transmission of drug-resistant HIV-1 variants.[10] The development of new PIs that address this issue is essential to the future management of HIV/AIDS.

Molecular Insight and Design Strategies To Combat Drug Resistance

Our structural analysis and comparison of protein–ligand X-ray structures of wild-type and mutant HIV proteases have revealed that the active site backbone conformation of mutant proteases is only minimally distorted.[11,12] This molecular insight led us to presume that an inhibitor which makes maximum interactions in the active site of HIV protease, particularly extensive hydrogen-bonding interactions in the protein backbone of the wild-type enzyme, will also retain these key interactions in the active site of mutant proteases. Our structure-based design to combat drug resistance is guided by the premise that an inhibitor exhibiting extensive hydrogen-bonding interactions with the protein backbone of the wild-type enzyme will likely retain potency against the mutant strains, since the mutations cannot easily eliminate the backbone interactions. Our objective is then focused on designing inhibitors that specifically target and maximize these interactions with backbone atoms. Another critical issue of current HAART therapies is the poor bioavailability of the current PIs. This in turn is responsible for much of the high-dose-related severe side effects and poor compliance issues.[13] Thus, our design of ligands and templates is also focused on designing non-peptidic cyclic/heterocyclic structures with improved bioavailability. Of particular interest, we plan to design cyclic ether or polyether-derived templates as these features are common to biologically active natural products. Such polyether templates may help improving aqueous solubility and increase oral bioavailability of PIs.

Development of Bis-THF as a High-Affinity P_2 Ligand

In a preliminary investigation based upon the X-ray structure of saquinavir-bound HIV-1 protease,[14] we designed a conformationally constrained cyclic ether-derived ligand to mimic the asparagine carbonyl binding in the S_2 subsite. As shown in Figure 1, inhibitor **1** with a 3(*S*)-tetrahydrofuranylurethane displayed an enzyme IC_{50} of 132 nM. The corresponding 3(*R*)-tetrahydrofuranyl derivative was significantly less potent (enzyme IC_{50} of 694 nM).[15,16] The potency-enhancing effect of 3(*S*)-tetrahydrofuran was further demonstrated in inhibitor **2** with a hydroxylethylene isostere.[16] Subsequently, this 3(*S*)-tetrahydrofuran was incorporated in an (*R*)-(hydroxyethyl)sulfonamide isostere to provide **3** (VX-476). This low-molecular-weight protease inhibitor was later approved by the FDA as amprenavir for the treatment of AIDS.[17]

A preliminary protein–ligand X-ray crystal structure of **1**-bound HIV-1 protease indicated that the oxygen atom of the tetrahydrofuran ring may be involved in a weak interaction with the backbone NHs of Asp 29 and Asp 30.[18] In an effort to further improve the potency of inhibitor **1**, we speculated that a fused bicyclic tetrahydrofuran (bis-THF) could effectively interact with both Asp 29 and Asp 30

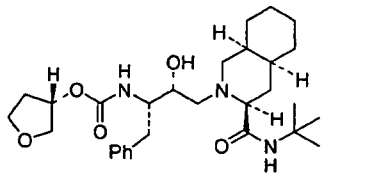

1 IC_{50} = 132 nM
CIC_{95} = 800 nM

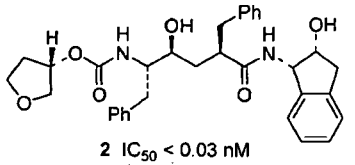

2 IC_{50} < 0.03 nM
CIC_{95} = 3 nM

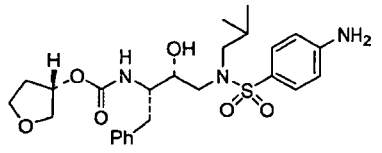

3 Ki = 0.6 nM
IC_{90} = 40 nM

FIGURE 1. Cyclic ether-containing protease inhibitors.

amide NHs. Furthermore, the bicyclic rings of the bis-THF should offset loss of the P_3-hydrophobic quinoline ring of saquinavir. Interestingly, the bis-THF template is a subunit of ginkgolides A–C, an important class of natural products with significant biological activities.[19] Chemistry and biology of ginkgolides provided strong motivation for designing ginkgolide-derived ligands for the HIV protease substrate binding site.[19–21] Indeed, inhibitor **4** with a (3*R*,3a*S*,6a*R*)-bis-THF urethane showed a significant improvement in potency compared to **1** and its corresponding (*R*)-derivative (**5**).[15] Inhibitor **4** exhibited excellent enzyme inhibitory and antiviral potency (Figure 2).

Incorporation of the bis-THF ligand improved aqueous solubility and reduced molecular weight. Our systematic structure–activity relationship studies also ascertained that the stereochemistry (see inhibitor **5**, Figure 2), position of both oxygens (see inhibitors **6** and **7**, Figure 3), and ring sizes were critical to the activity of the inhibitor. An X-ray structure of **4**-bound HIV-1 protease revealed that both oxygens of the bis-THF ligand are within hydrogen-bonding distance to the Asp 29 and Asp 30 amide NHs in the S_2 subsite.[15]

Synthesis of the Bis-THF Ligand

The multistep synthesis of the optically active bis-THF ligand starting from (*R*)-malic acid was ineffective for the preparation of structural variants. We thus developed a three-step synthesis of racemic bis-THF followed by an immobilized lipase-catalyzed

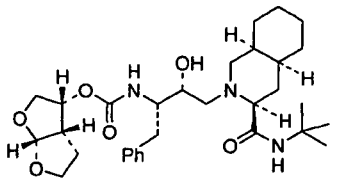

4 IC_{50} = 1.8 nM
CIC_{95} = 46 nM

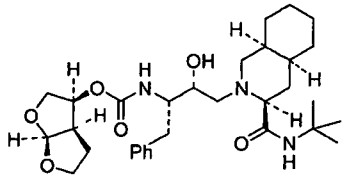

5 IC_{50} = 6.4 nM
CIC_{95} = 200 nM

FIGURE 2. Bis-THF-containing protease inhibitors.

enzymatic resolution to provide optically active (3*R*,3a*S*,6a*R*)-3-hydroxyhexahydrofuro[2,3-*b*]furan (**12**) in high enantiomeric excess (>96% ee), as shown in Scheme 1. This synthesis helped us to extend the scope and utility of this privileged polyether-like non-peptidic ligand.[22] We recently reported two optically active syntheses of this ligand (Scheme 2). The first synthesis involved a novel stereoselective photochemical 1,3-dioxolane addition to 5(*S*)-benzyloxymethyl-2(5*H*)-furanone as the key step. The corresponding furanone was prepared in high enantiomeric excess by a lipase-catalyzed selective acylation of **15** followed by ring-closing olefin metathesis.[23] The second synthesis utilizes an ester-derived Ti–enolate-based highly stereoselective *anti*-aldol reaction as the key step.[24]

Development of Darunavir

We investigated the potency-enhancing effect of the bis-THF ligand with other isosteres. Incorporation of bis-THF in (*R*)-hydroxyethyl(sulfonamide) isosteres led to several exceedingly potent PIs with marked antiviral potency and drug-resistance profiles, as shown in Figure 4.[25]

Inhibitor **17** with a *p*-methoxysulfonamide as the P_2' ligand exhibited very impressive enzyme potency and antiviral activity. This PI has shown an excellent drug-resistance profile and good pharmacokinetic properties in laboratory animals.[26,27] It was later renamed TMC-126. In fact, inhibitor **17** showed >10-fold higher potency than the five currently available PIs (i.e., ritonavir (RTV), indinavir (IDV), saquinavir (SQV), nelfinavir (NFV), and amprenavir (APV)) in drug-sensitivity assays. It's IC_{50}s consistently remained as low as 0.3 nM.[26,27] Inhibitor **17** also displayed an unprecedented broad-spectrum activity against a large panel of primary, multidrug-resistant HIV-1 strains.[27]

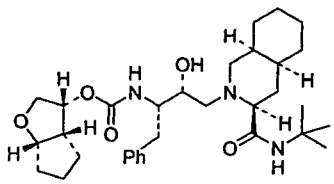

6 IC_{50} = 190 nM

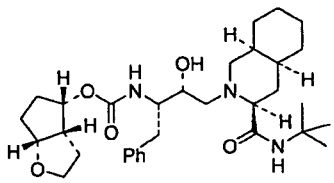

7 IC_{50} = 17 nM

FIGURE 3. Structure of inhibitors **6** and **7**.

SCHEME 1. Efficient Optically Active Synthesis of Bis-THF Ligand

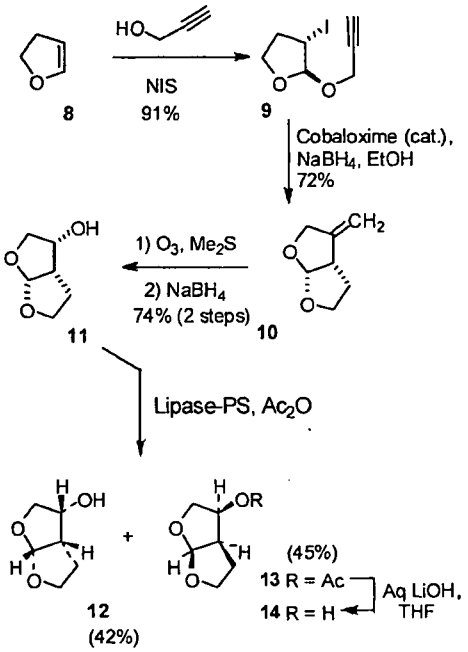

Incorporation of bis-THF into a *p*-aminosulfonamide isostere led to inhibitor **18**. Inhibitor **18** also showed unprecedented antiviral activity and outperformed most of the other currently available PIs against HIV-1_{Ba-L} by a 6–13-fold difference in IC_{50} values (Table 1).[28] Furthermore, this PI suppressed the replication of HIV-2 isolates with the most potent activity. It was later renamed TMC-114 or darunavir. When tested against HIV-1 strains that were selected for resistance to SQV, APV, IDV, NFV, or RTV after exposure to the various PIs at different concentrations (up to 5 μM), inhibitor **18** consistently and effectively suppressed viral infectivity and replication (IC_{50} values 0.003–0.029 μM) (Table 2), although lower activity was observed with APV-resistant strains (IC_{50} = 0.22 μM). In addition, inhibitor **18** potently blocked the replication of seven multidrug-resistant HIV-strains, isolated from heavily drug experienced patients with 9–14 mutations evidenced in their protease-encoding region.[28] Subsequent studies using a large panel of HIV-1 mutant strains provided further evidence of the remarkable profile of this inhibitor.[29]

SCHEME 2. Stereoselective Syntheses of the Bis-THF Ligand

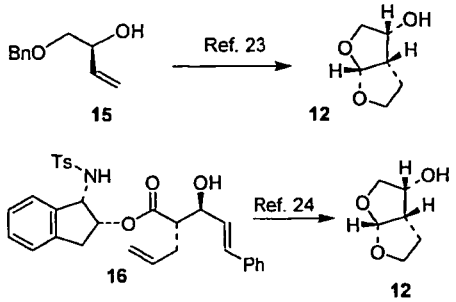

X-ray Crystal Structure of Darunavir and Evidence of Backbone Binding

High-resolution (1.10–1.34 Å) X-ray crystal structures of inhibitor **18** complexed with either wild-type HIV-1 protease or with two mutant proteases consistently showed strong hydrogen bonding of the bis-THF oxygens with the two Asp 29 and Asp 30 backbone amides (Figure 5).[28,30] New polar interactions with the Asp 30 side-chain carboxylate were also observed.[30] Additional hydrogen bonds were observed between the aniline moiety and the carbonyl oxygen and side-chain carboxylate of Asp 30′. Subsequent crystal structures of **18**-bound mutant proteases, including inhibitor **18**-bound resistant protease, clearly displayed a similar hydrogen-bonding pattern around the bis-THF ligand. These interactions seem to be crucial for maintaining the high affinity of the inhibitor

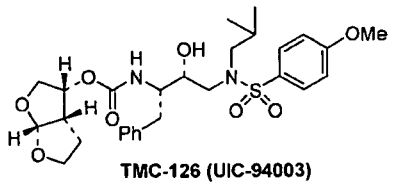

TMC-126 (UIC-94003)

17 K_i = 14 pM
IC_{90} = 1.4 nM

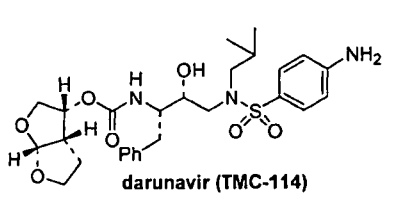

darunavir (TMC-114)

18 K_i = 16 pM
IC_{90} = 4.1 nM

FIGURE 4. Bis-THF-Derived Protease Inhibitors.

TABLE 1. Sensitivities of Selected Anti-HIV Agents against HIV-1_{Ba-L}, HIV-2_{ROD}, and HIV-2_{EHO}

		PIs, mean IC_{50} (nM) ± SDs[a]						
virus	cell type	AZT	SQV	APV	IDV	NFV	RTV	18 (TMC-114)
HIV-1_{Ba-L}[b]	PBMC	9 ± 1	18 ± 10	26 ± 5	25 ± 12	17 ± 4	39 ± 20	3 ± 0.3
HIV-2_{ROD}[c]	MT-2	18 ± 2	3 ± 0.2	230 ± 10	14 ± 6	19 ± 3	130 ± 60	3 ± 0.1
HIV-2_{EHO}[c]	MT-2	11 ± 2	6 ± 2	170 ± 50	11 ± 2	29 ± 18	240 ± 6	6 ± 3

[a] All assays were conducted in duplicate or triplicate; the data represent IC_{50} mean values (±SD) derived from the result of three independent experiments. [b] IC_{50} were evaluated with PHA–PBMC and the inhibition of p24 Gag protein production by the drug as an end point. [c] MT-2 cells were exposed to the virus and cultured, and IC_{50} values were determined by MTT assay.

TABLE 2. Activity of 18 against Laboratory PI-Resistant HIV-1

		IC_{50} (μM)[b]					
virus	amino acid substitution[a]	SQV	APV	IDV	NFV	RTV	18 (TMC-114)
HIV-1_{NL4-3}	wild type	0.009 (1)	0.027 (1)	0.011 (1)	0.020 (1)	0.018 (1)	0.003 ± 0.0005 (1)
HIV-$1_{SQV5\mu M}$	L10I, G48V, I54V, L90M	>1 (>111)	0.17 (6)	>1 (>91)	0.30 (15)	>1 (>56)	0.005 ± 0.0009 (2)
HIV-$1_{APV5\mu M}$	L10F, V32I, M46I, I54M, A71V, I84V	0.020 (2)	>1 (>37)	0.31 (28)	0.21 (11)	>1 (>56)	0.22 ± 0.05 (73)
HIV-$1_{IDV5\mu M}$	L10F, L24I, M46I, L63P, A71V, G73S, V82T	0.015 (2)	0.33 (12)	>1 (>91)	0.74 (37)	>1 (>56)	0.029 ± 0.0007 (10)
HIV-$1_{NFV5\mu M}$	L10F, D30N, K45I, A71V, T74S	0.031 (3)	0.093 (3)	0.28 (25)	>1 (>50)	0.09 (5)	0.003 ± 0.0002 (1)
HIV-$1_{RTV5\mu M}$	M46I, V82F, I84V	0.013 (1)	0.61 (23)	0.31 (28)	0.24 (12)	>1 (>56)	0.025 ± 0.006 (8)

[a] In PR. [b] MT-4 cells (10^4) were exposed to each HIV-1 (100x$TCID_{50}$s), and the inhibition of p24 Gag protein production by the drug was used as an end point. Numbers in parentheses represent the fold changes of IC_{50}s for each isolate relative to that of HIV-1_{NL4-3}.

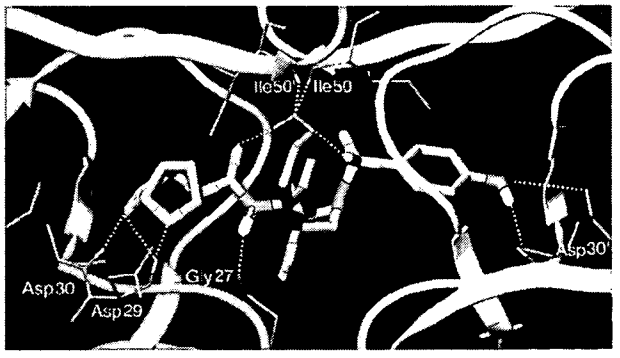

FIGURE 5. Interactions in X-ray crystal structure of **18**-bound HIV protease.

for the protease and appear to provide an explanation for the high potency against mutant proteases.[31–33]

Clinical Development of Darunavir

Inhibitor **18**, later renamed darunavir, showed a favorable pharmacokinetic profile in laboratory animals and was subsequently selected for further clinical studies. Tibotec (Belgium) carried out clinical developments of darunavir (**18**).[34] Darunavir (DRV) showed superior pharmacokinetic properties when coadministered with low doses of ritonavir.[35] Two-phase IIB clinical trials, POWER 1 and 2, are currently being performed on treatment-experienced patients to assess the safety, tolerability, and efficacy of darunavir with low doses of ritonavir (DRV/r) for 144 weeks. Early results at 24 weeks for one trial (POWER 1) showed that 77% of the DRV/r group vs. 25% for the control PI group achieved a ≥1 $\log_{10}$ viral load reduction, 53% under DRV/r vs. 18% reached a <50 cop-

TABLE 3. Sensitivity of HIV-1_{LAI} and HIV-1_{Ba-L} against New PIs

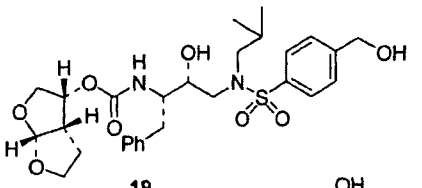

19

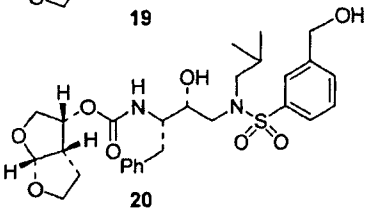

20

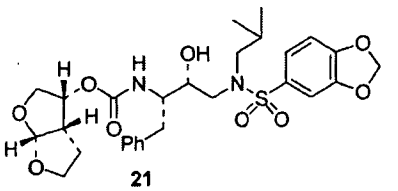

21

			IC_{50} (nm)		
virus	cell type	assay	**19**	**20**	**21**
HIV-1_{LAI}[a]	MT-2	MTT	5.3	28	0.22
HIV-1_{LAI}[b]	PBMC	p24	2.7	8	0.22
HIV-1_{Ba-L}[b]	PBMC	p24	3	9.3	0.33

[a] MT2 cells (2×10^3) were exposed to 100$TCID_{50}$ of HIV-1_{LAI} culture at various concentrations of PIs. [b] The IC_{50} values were determined by exposing the PHA-stimulated PBMC to the HIV-1 strain (50$TCID_{50}$ dose per 1×10^6 PBMC) at various concentrations of PI.

TABLE 4. Activity and Cross-Resistance Profile of Inhibitor 21

virus[a]	EC_{50} (nM)					
	SQV	RTV	NFV	APV	DRV	21 (GRL-98065)
$HIV\text{-}1_{ERS104pre}$ (wild-type X_4)	8 ± 3	25 ± 5	15 ± 4	29 ± 5	3.8 ± 0.7	0.5 ± 0.2
$HIV\text{-}1_{MDR/TM\ (X4)}$	180 ± 50 (23)	>1000 (>40)	>1000 (>67)	300 ± 40 (10)	4.3 ± 0.7 (1)	3.2 ± 0.6 (6)
$HIV\text{-}1_{MDR/MM\ (R5)}$	140 ± 40 (18)	>1000 (>40)	>1000 (>67)	480 ± 90 (17)	16 ± 7 (4)	3.8 ± 0.6 (8)
$HIV\text{-}1_{MDR/JSL\ (R5)}$	290 ± 50 (36)	>1000 (>40)	>1000 (>67)	430 ± 50 (15)	27 ± 9 (7)	6 ± 2 (12)
$HIV\text{-}1_{MDR/B\ (X4)}$	270 ± 60 (34)	>1000 (>40)	>1000 (>67)	360 ± 90 (12)	40 ± 10 (11)	3.9 ± 0.5 (8)
$HIV\text{-}1_{MDR/C\ (X4)}$	35 ± 4 (4)	>1000 (>40)	420 ± 60 (28)	250 ± 50 (9)	9 ± 5 (2)	2.7 ± 0.3 (5)
$HIV\text{-}1_{MDR/G\ (X4)}$	33 ± 5 (4)	>1000 (>40)	370 ± 50 (25)	320 ± 20 (11)	7 ± 5 (2)	3.4 ± 0.3 (7)

[a] The amino acid substitutions identified in the protease-encoding region compared to the consensus type B sequence cited from the Los Alamos database include L63P in HIV-1ERS104pre; L10I, K14R, R41K, M46L, I54V,L63P, A71V, V82A, L90M, I93L in HIV-1MDR/TM; L10I, K43T, M46L, I54V, L63P, A71V, V82A, L90M, and Q92K in HIV-1 MDR/MM; L10I, L24I, I33F, E35D, M36I, N37S, M46L, I54V, R57K, I62V, L63P, A71V, G73S, and V82A in HIV-1 MDR/JSL; L10I, K14R, L33I, M36I, M46I, F53I, K55R, I62V, L63P, A71V, G73S, V82A, L90M, and I93L in HIV-1 MDR/B; L10I, I15V, K20R, L24I, M36I, M46L, I54V, I62V, L63P, K70Q, V82A, and L89 M in HIV-1 MDR/C; and L10I, V11I, T12E, I15V, L19I, R41K, M46L, L63P, A71T, V82A, and L90 M in HIV-1 MDR/G. HIV-1ERS104 preserved as a source of wild-type HIV-1.

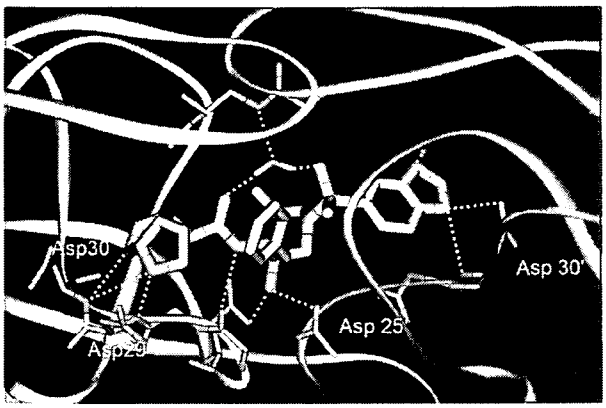

FIGURE 6. Crystal structure of inhibitor **21**-bound HIV-1 protease.

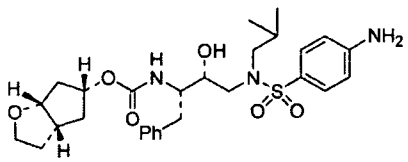

22 K_i = 0.14±0.02 nM
IC_{90} = 8 nM

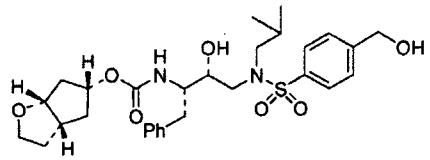

23 K_i = 0.0045±0.001 nM
IC_{90} = 1.8 nM

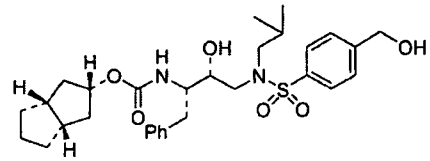

24 K_i = 5.3±0.3 nM
IC_{90} >1000 nM

FIGURE 7. Structures of inhibitors **22–24**.

ies/mL viral load, CD_4+ cell count increased from baseline by 124 cells/mL in the DRV/r arm vs. 20 cells in the others.[36] A recent report at week 48 for the two trials showed that 61%

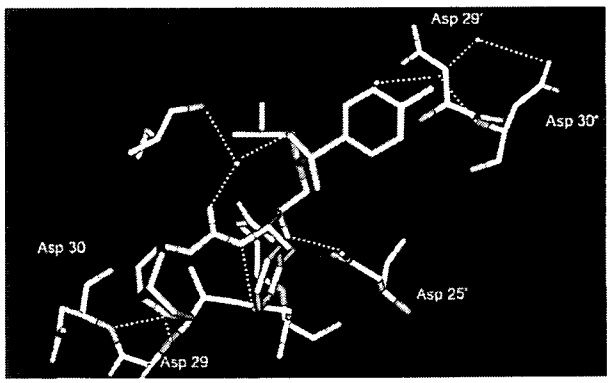

FIGURE 8. Inhibitor **23**-bound X-ray structure of HIV-1 protease.

of patients under DRV/r (600mg/100mg twice daily) maintained a >1 log_{10} reduction of viral load vs. baseline compared to 15% with the control PI arms.[37] Most impressively, 45% presented <50 viral copies/mL as opposed to 10% for the control arm. Darunavir was approved by the FDA in June 2006, as the first treatment for drug-resistant HIV.[38]

Bis-THF-Derived Novel PIs

We have further explored a number of P_2' sulfonamide functionalities to interact with the backbone atoms in the S_2' subsite. As shown in Table 3, inhibitors **19–21** displayed exceedingly potent inhibitory properties. Inhibitor **21**, which contains a benzodioxolanesulfonamide derivative as its P_2' ligand, provided impressive enzyme inhibitory (<5 pM) and antiviral potency.[39] The antiviral activity of the inhibitors was evaluated against wild-type clinical isolates $HIV\text{-}1_{LAI}$ and $HIV\text{-}1_{Ba\text{-}L}$ in PBMC cells and $HIV\text{-}1_{LAI}$-exposed MT-2 cells. Results of drug sensitivities are summarized in Table 3. Inhibitor **21**(GRL-98065) was then evaluated against both wild-type and HIV-1 mutant strains.[39] As shown in Table 4, inhibitor **21** outperformed most of the currently available PIs against multidrug-resistant HIV-1 clinical isolates, including DRV by a 2 to 10-fold improvement of activity.[39] Additional studies on

TABLE 5. Activity of 23 against a Wide Spectrum of HIV-1 Mutant Isolates

virus	mutations[a]	IC_{50} (nM) values						
		SQV	RTV	IDV	NFV	APV	DRV	**23**
1 (ET)	L10I	17	15	30	32	23	nd	3
2 (B)	L10I, K14R, L33I, M36I, M46I, F53L, K55R, I62V, L63P, A71V, G73S, V82A, L90M, I93L	230	>1000	>1000	>1000	290	10.2	15
3 (C)	I10L, I15V, K20R, M36I, M46L, I54V, K55R, I62V, L63P, K70Q, V82A, L89M	100	>1000	500	310	300	3.5	5
4 (G)	L10I, V11I, T12E, I15V, L19I, R41K, M46L, L63P, A71T, V82A, L90M	59	>1000	500	170	310	3.7	20
5 (TM)	L10I, K14R, R41K, M46L, I54V, L63P, A71V, V82A, L90M, I93L	250	>1000	>1000	>1000	220	3.5	4
6 (EV)	L10V, K20R, L33F, M36I, M46I, I50V, I54V, D60E, L63P, A71V, V82A, L90M	>1000	>1000	>1000	>1000	>1000	n.d.	52
7 (ES)	L10I, M46L, K55R, I62V, L63P, I72L, G73C, V77I, I84V, L90M	>1000	>1000	>1000	>1000	>1000	n.d.	31
8 (K)	L10F, D30N, K45I, A71V, T74S	20	57	260	>1000	68	3	3

[a] Amino acids substitutions identified in the protease-encoding region of HIV-1_{ET} (ET), HIV-1_B (B), HIV-1_C (C), HIV-1_G (G), HIV-1_{TM} (TM), HIV-1_{EV} (EV), HIV-1_{ES} (ES), HIV-1_K (NFV_R) as compared to consensus B sequence cited from the Los Alamos database.

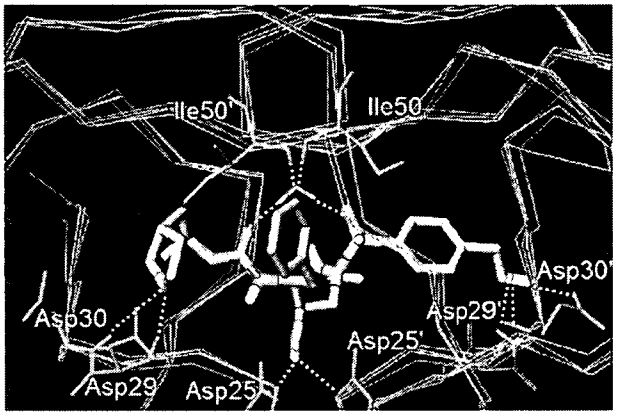

FIGURE 9. Inhibitor **23**-bound to the active site of wild-type HIV-1 protease superimposed upon the three most highly mutated drug-resistant proteases.

PI-resistant HIV-1 viral strains showed little sign of cross-resistance with inhibitor **21.**

As shown in Figure 6, the protein–ligand X-ray crystal structure of **21** revealed a pattern of four hydrogen-bonding interactions with the backbone residues of the protease similar to darunavir.[39] Because of its intriguing potency-enhancing effect and also its ability to maintain high potency against multidrug-resistant viral strains, the bis-THF ligand has been utilized for the development of other potent PIs. Most notably, researchers at GlaxoSmithKline explored an extremely potent inhibitor named brecanavir, which was a structural variant of inhibitor **21**.[40] The clinical development of this inhibitor was later abandoned reportedly due to difficulties in its formulation.

Design of Hexahydrocyclopentanofuranyl Ligand Based upon the "Backbone Binding" Concept

The remarkable ability of bis-THF-derived PIs to combat drug resistance has been documented through the clinical development of darunavir. Numerous protein–ligand X-ray crystal structures of bis-THF-containing PIs have now provided ample evidence of our concept that inhibitors with strong hydrogen-bonding interactions with the backbone atoms in the protease active site will be likely to maintain these interactions with mutant proteases and effectively combat drug resistance.[30–32] We next sought to design and develop PIs containing other novel ligands that could extensively interact with the backbone atoms. As outlined in Figure 7, we designed inhibitors **22** and **23** that contain a stereochemically defined bicyclic hexahydrocyclopentanofuran as a P_2 ligand.[41]

As shown, inhibitor **22**, with a 4-aminophenylsulfonamide as the P_2' ligand, exhibited very good enzyme inhibitory and antiviral activity. We then introduced a hydroxymethylphenylsulfonamide as a P_2' sulfonamide moiety with the intention of promoting hydrogen bonds between the hydroxyl oxygen and suitable backbone atoms in the S_2' subsite. Inhibitor **23** with a P_2' hydroxymethylphenylsulfonamide provided an impressive K_i value of 4.5 pM and antiviral IC_{50} of 1.8 nM. Compound **24** exhibited a >1100-fold loss of activity compared to that of inhibitor **23**, indicating the importance of the cyclopentanofuranyl oxygen's critical interactions in the active site. The X-ray crystal structure of **23**-bound HIV-1 protease (Figure 8) reveals that the P_2 ligand oxygen forms hydrogen bonding with the Asp 29 backbone NH.[41] The hydroxymethyl group of the P_2' sulfonamide moiety is within hydrogen-bonding distance to the Asp 30' NH as well as the side-chain carboxylate (through a 10–20° rotation of the αC–βC bond of the residue).

Inhibitor **23** has shown very impressive antiviral activity against a panel of multidrug-resistant HIV-1 variants, and the results are shown in Table 5. It exerted high potency against six other variants with IC_{50} values ranging from 4 to 52 nM.[41] All the currently available protease inhibitors tested were

highly resistant to clinical strains. Overall, inhibitor **23** is highly active against a wide spectrum of drug-resistant variants and its activity is comparable to that of darunavir.

We have compared the X-ray structure of **23** with several reported protein–ligand X-ray structures of mutant proteases. A least-squares fit of the protease α-carbons atoms was performed, allowing comparison of the interactions of **23** with each of the mutant proteases. Figure 9 depicts the superimposition of the X-ray structure of **23** with the three most highly mutated drug-resistant proteases (PDB code and color: 2F81[41] with wild type, red; 2FDD,[42] blue; 1SGU,[43] green; 1HSH,[44] yellow). As can be seen, despite multiple mutations, there is only small change in active site backbone positions. Both the P_2 ligand oxygen and the P_2' hydroxymethyl group are within hydrogen-bonding distance to the respective backbone atoms and side-chain residues in the enzyme active site. On the basis of this analysis, it appeared that inhibitor **23** should retain good to excellent contacts with the backbone of mutant proteases.

Conclusion

The emergence of drug resistance to current antiretroviral treatment represents a major challenge that needs to be addressed with the development of a new generation of inhibitors with improved pharmacological profiles. Our structure-based design of new generation protease inhibitors incorporating novel cyclic-ether-derived ligands provided exceedingly potent inhibitors with impressive drug-resistance profiles. The inhibitors are designed to make extensive interactions, particularly hydrogen bonding, with the protein backbone of HIV-1 protease. Our extensive structural analysis of protein–ligand X-ray structures of bis-THF-containing inhibitors with wild-type and mutant proteases revealed retention of strong hydrogen-bonding interactions with the protein backbone. This structural element is only slightly distorted despite multiple amino acid mutations in the active site of HIV protease. One of our designed inhibitors, darunavir, has shown superior activity against multi-PI-resistant variants compared to other FDA-approved inhibitors. It has been recently approved as the first treatment of drug-resistant HIV. This important design concept targeting the active site protein backbone may serve as an effective strategy to combat drug resistance.

Financial support by the National Institutes of Health (GM 53386, AKG) is gratefully acknowledged. This work was also supported in part by the Intramural Research Program of the Center for Cancer Research, National Cancer Institute, National Institutes of Health, and in part by a Grant-in-aid for Scientific Research (Priority Areas) from the Ministry of Education, Culture, Sports, Science, and Technology of Japan (Monbu Kagakusho) and a Grant for Promotion of AIDS Research from the Ministry of Health, Welfare, and Labor of Japan. We also thank Dr. Geoff Bilcerand and Mr. Xiaoming Xu for helpful suggestions.

BIOGRAPHICAL INFORMATION

Arun K. Ghosh received his Ph.D. from the University of Pittsburgh and pursued postdoctoral research with Professor E. J. Corey at Harvard University. He was a Professor of Chemistry at the University of Illinois at Chicago from 1994 to 2005. From 2005 to present, he is a Professor in the departments of chemistry and medicinal chemistry at Purdue University.

Bruno D. Chapsal obtained his M.S. in chemistry from CPE Lyon, France, and received his Ph.D. from Stony Brook University, NY, under the direction of Professor Iwao Ojima. He is currently carrying out postdoctoral research in Professor Ghosh's laboratories.

Irene T. Weber received her Ph.D. from the University of Oxford, England, under the supervision of Professor Louise Johnson. She pursued postdoctoral research with Professor Thomas Steitz at Yale University. She was Professor of Microbiology and Immunology at Thomas Jefferson University in Philadelphia from 1991 to 2000. From 2001 to the present she is Professor of Biology and Chemistry at Georgia State University in Atlanta.

Hiroaki Mitsuya received his M.D. and Ph.D. from the Kumamoto University School of Medicine, Japan. He was a Visiting Scientist at the National Cancer Institute from 1982 to 1990. From 2001 to present, he is Principal Investigator & Chief, Experimental Retrovirology Section, HIV and AIDS Malignancy Branch, National Cancer Institute, Bethesda, MD. From 1997 to present, he is also Professor of Medicine and Chairman, Department of Internal Medicine, Kumamoto University School of Medicine, Japan.

FOOTNOTES

*To whom correspondence should be addressed. Fax: 765-496-1612. E-mail: akghosh@purdue.edu.

REFERENCES

1 Barre-Sinoussi, F.; Chermann, J. C.; Rey, F.; Nugeyre, M. T.; Chamaret, S.; Gruest, J.; Dauguet, C.; Axler-Blin, C.; Vezinet-Brun, F.; Rouzioux, C.; Rozenbaum, W.; Montagnier, L. Isolation of a T-lymphotropic Retrovirus from a Patient at Risk for Acquired Immune Deficiency Syndrome (AIDS). *Science* **1983**, *220*, 868–871.

2 Gallo, R. C.; Salahuddin, S. Z.; Popovic, M.; Shearer, G. M.; Kaplan, M.; Haynes, B. F.; Palker, T. J.; Redfield, R.; Oleske, J.; Safai, B.; White, G.; Foster, P.; Markham, P. D. Frequent Detection and Isolation of Cytopathic Retroviruses (HTLV-III) from Patients with AIDS and at Risk for AIDS. *Science* **1984**, *224*, 500–503.

3 The Impact of AIDS on People and Societies/2006, report on the Global AIDS Epidemic, http://data.unaids.org/pub/GlobalReport/2006/2006_GR_CH04_en.pdf

4 De Clercq, E. New Approaches toward Anti-HIV Chemotherapy. *J. Med. Chem.* **2005**, *48*, 1297–1313.

5 Graves, M. C.; Lim, J. J.; Heimer, E. P.; Kramer, R. A. An 11-kDa Form of Human Immunodeficiency Virus Protease Expressed in Escherichia Coli is Sufficient for Enzymatic Activity. *Proc. Natl. Acad. Sci. U.S.A.* **1988**, *85*, 2449–2453.

6 Wlodawer, A.; Vondrasek, J. Inhibitors of HIV-1 Protease: A Major Success of Structure-Assisted Drug Design. *Annu. Rev. Biophys. Biomol. Struct.* **1998**, *27*, 249–284.

7 The First HIV Protease Inhibitors Approved by FDA. *Antiviral Agents Bull.* **1995**, *8*, 353–355.

8 Sepkowitz, K. A. AIDS—The First 20 Years. *N. Engl. J. Med.* **2001**, *344*, 1764–1772.

9 Grabar, S.; Pradier, C.; Le Corfec, E.; Lancar, R.; Allavena, C.; Bentata, M.; Berlureau, P.; Dupont, C.; Fabbro-Peray, P.; Poizot-Martin, I.; Costagliola, D. Factors Associated with Clinical and Virological Failure in Patients Receiving a Triple Therapy Including a Protease Inhibitor. *AIDS* **2000**, *14*, 141–149.

10 Wainberg, M. A.; Friedland, G. Public Health Implications of Antiretroviral Therapy and HIV Drug Resistance. *J. Am. Med. Assoc.* **1998**, *279*, 1977–1983.

11 Hong, L.; Zhang, X.; Hartsuck, J. A.; Tang, J. Crystal Structure of an In Vivo HIV-1 Protease Mutant in Complex with Saquinavir: Insights Into the Mechanisms of Drug Resistance. *Protein Sci.* **2000**, *9*, 1898–1904.

12 Laco, G. S.; Schalk-Hihi, C.; Lubkowski, J.; Morris, G.; Zdanov, A.; Olson, A.; Elder, J. H.; Wlodawer, A.; Gustchina, A. Crystal Structures of the Inactive D30N Mutant of Feline Immunodeficiency Virus Protease Complexed with a Substrate and an Inhibitor. *Biochemistry* **1997**, *36*, 10696–10708.

13 Glesby, M. J. Toxicities and Adverse Effects of Protease Inhibitors. In *Protease Inhibitors in AIDS Therapy*; Ogden, R. C., Flexner, C. W., Eds.; Marcel Dekker: New York, 2001; pp 237–256.

14 Krohn, A.; Redshaw, S.; Ritchie, J. C.; Graves, B. J.; Hatada, M. H. Novel Binding Mode of Highly Potent HIV-Proteinase Inhibitors Incorporating the (R)-Hydroxyethylamine Isostere. *J. Med. Chem.* **1991**, *34*, 3340–3342.

15 Ghosh, A. K.; Kincaid, J. F.; Walters, D. E.; Chen, Y.; Chaudhuri, N. C.; Thompson, W. J.; Culberson, C.; Fitzgerald, P. M. D.; Lee, H. Y.; McKee, S. P.; Munson, P. M.; Duong, T. T.; Darke, P. L.; Zugay, J. A.; Schleif, W. A.; Axel, M. G.; Lin, J.; Huff, J. R. Nonpeptidal P_2 Ligands for HIV Protease Inhibitors: Structure-Based Design, Synthesis, and Biological Evaluation. *J. Med. Chem.* **1996**, *39*, 3278–3290.

16 Ghosh, A. K.; Thompson, W. J.; McKee, S. P.; Duong, T. T.; Lyle, T. A.; Chen, J. C.; Darke, P. L.; Zugay, J. A.; Emini, E. A.; Schleif, W. A.; Huff, J. R.; Anderson, P. S. 3-Tetrahydrofuran and Pyran Urethanes as High-Affinity P_2-Ligands for HIV-1 Protease Inhibitors. *J. Med. Chem.* **1993**, *36*, 292–294.

17 Kim, E. E.; Baker, C. T.; Dwyer, M. D.; Murcko, M. A.; Rao, B. G.; Tung, R. D.; Navia, M. A. Crystal Structure of HIV-1 Protease In Complex with VX-478, a Potent and Orally Bioavailable Inhibitor of the Enzyme. *J. Am. Chem. Soc.* **1995**, *117*, 1181–1182.

18 Ghosh, A. K.; Thompson, W. J.; Fitzgerald, P. M. D.; Culberson, J. C.; Axel, M. G.; McKee, S. P.; Huff, J. R.; Anderson, P. S. Structure-based Design of HIV-1 Protease Inhibitors: Replacement of two Amides and a 10π-Aromatic System by a Fused Bis-Tetrahydrofuran. *J. Med. Chem.* **1994**, *37*, 2506–2508.

19 Nakanishi, K. The Ginkgolides. *Pure Appl. Chem.* **1967**, *14*, 89–114.

20 Corey, E. J.; Kang, M. C.; Desai, M. C.; Ghosh, A. K.; Houpis, I. N. Total Synthesis of (+/−)-Ginkgolide-B. *J. Am. Chem. Soc.* **1988**, *110*, 649–651.

21 Corey, E. J.; Ghosh, A. K. Total Synthesis of Ginkgolide A. *Tetrahedron Lett.* **1988**, *29*, 3205–3206.

22 Ghosh, A. K.; Chen, Y. Synthesis and Optical Resolution of High Affinity P_2 Ligands for HIV-1 Protease Inhibitors. *Tetrahedron Lett.* **1995**, *36*, 505–508.

23 Ghosh, A. K.; Leschenko, S.; Noetzel, M. Stereoselective Photochemical 1,3-Dioxolane Addition to 5-Alkoxymethyl-2(5*H*)-furanone: Synthesis of Bis-Tetrahydrofuranyl Ligand for HIV Protease Inhibitor UIC-94017 (TMC-114). *J. Org. Chem.* **2004**, *69*, 7822–7829.

24 Ghosh, A. K.; Li, J.; Sridhar, P. R. A Stereoselective Anti-Aldol Route to (3*R*,3a*S*,6a*R*)-Hexahydrofuro[2,3-*b*]furan-3-ol: A Key Ligand for a New Generation of HIV Protease Inhibitors. *Synthesis* **2006**, *18*, 3015–3018.

25 Ghosh, A. K.; Kincaid, J. F.; Cho, W.; Walters, D. E.; Krishnan, K.; Hussain, K. A.; Koo, Y.; Cho, H.; Rudall, C.; Holland, L.; Buthod, J. Potent HIV Protease Inhibitors Incorporating High-Affinity P_2-Ligands and (*R*)-(Hydroxyethylamino)sulfonamide Isostere. *Bioorg. Med. Chem. Lett.* **1998**, *8*, 687–690.

26 Ghosh, A. K.; Pretzer, E.; Cho, H.; Hussain, K. A.; Duzgunes, N. Antiviral Activity of UIC-PI, a Novel Inhibitor of the Human Immunodeficiency Virus Type 1 Protease. *Antiviral Res.* **2002**, *54*, 29–36.

27 Yoshimura, K.; Kato, R.; Kavlick, M. F.; Nguyen, A.; Maroun, V.; Maeda, K.; Hussain, K. A.; Ghosh, A. K.; Gulnik, S. V.; Erickson, J. W.; Mitsuya, H. A Potent Human Immunodeficiency Virus Type 1 Protease Inhibitor, UIC-94003 (TMC-126), and Selection of a Novel (A28S) Mutation in the Protease Active Site. *J. Virol.* **2002**, *76*, 1349–1358.

28 Koh, Y.; Nakata, H.; Maeda, K.; Ogata, H.; Bilcer, G.; Devasamudram, T.; Kincaid, J. F.; Boross, P.; Wang, Y.-F.; Tie, Y.; Volarath, P.; Gaddis, L.; Harrison, R. W.; Weber, I. T.; Ghosh, A. K.; Mitsuya, H. Novel *bis*-Tetrahydrofuranylurethane-Containing Nonpeptidic Protease Inhibitor (PI) UIC-94017 (TMC114) with Potent Activity against Multi-PI-Resistant Human Immunodeficiency Virus In Vitro. *Antimicrob. Agents Chemother.* **2003**, *47*, 3123–3129.

29 De Meyer, S.; Azijn, H.; Surleraux, D.; Jochmans, D.; Tahri, A.; Pauwels, R.; Wigerinck, P.; de Bethune, M.-P. TMC114, a Novel Human Immunodeficiency Virus Type 1 Protease Inhibitor Active against Protease Inhibitor-Resistant Viruses, Including a Broad Range of Clinical Isolates. *Antimicrob. Agents Chemother.* **2005**, *49*, 2314–2321.

30 Tie, Y.; Boross, P. I.; Wang, Y.-F.; Gaddis, L.; Hussain, A. K.; Leshchenko, S.; Ghosh, A. K.; Louis, J. M.; Harrison, R. W.; Weber, I. T. High Resolution Crystal Structures of HIV-1 Protease with a Potent Non-Peptide Inhibitor (UIC-94017) Active against Multi-Drug-Resistant Clinical Strains. *J. Mol. Biol.* **2004**, *338*, 341–352.

31 Kovalevsky, A. Y.; Tie, Y.; Liu, F.; Boross, P. I.; Wang, Y.-F.; Leshchenko, S.; Ghosh, A. K.; Harrison, R. W.; Weber, I. T. Effectiveness of Nonpeptide Clinical Inhibitor TMC-114 on HIV-1 Protease with Highly Drug Resistant Mutations D30N, I50V, and L90M. *J. Med. Chem.* **2006**, *49*, 1379–1387.

32 Kovalevsky, A. Y.; Liu, F.; Leshchenko, S.; Ghosh, A. K.; Louis, J. M.; Harrison, R. W.; Weber, I. T. Ultra-High Resolution Crystal Structure of HIV-1 Protease Mutant Reveals Two Binding Sites for Clinical Inhibitor TMC114. *J. Mol. Biol.* **2006**, *363*, 161–173.

33 King, N. M.; Prabu-Jeyabalan, M.; Nalivaika, E. A.; Wigerinck, P.; de Bethune, M.-P.; Schiffer, C. A. Structural and Thermodynamic Basis for the Binding of TMC114 a Next-Generation Human Immunodeficiency Virus Type 1 Protease Inhibitor. *J. Virol.* **2004**, *78*, 12012–12021.

34 De Meyer, S.; Peters, M. Abstracts 533 and 620, 11th Conference on Retroviruses and Opportunistic Infections (CROI); Feb 8–11 2004, San Francisco, CA.

35 Hoetelmans, R.; van der Sandt, I.; De Pauw, M.; Struble, K.; Peeters, M.; van der Geest, R. TMC114, a Next Generation HIV Protease Inhibitor: Pharmacokinetics and Safety Following Oral Administration of Multiple Doses with or without Low Doses of Ritonavir in Healthy Volunteers; Abstract 549, 10th Conference on Retroviruses and Opportunistic Infections (CROI); Feb 2003, Boston, MA.

36 Katlama, C.; Carvalho, M. T. M.; Cooper, D.; De Backer, K.; Lefebvre, E.; Pedro, R.; Rombouts, K.; Stoehr, A.; Vangeneugden, T.; Woehrmann, A. TMC114/r Outperforms Investigators-selected PI(s) in 3-class-experienced Patients: Week 24 Efficacy Analysis of POWER 1 (TMC114-C213) [Poster WeOaIB0102], 3rd IAS Conference on HIV Pathogenesis and Treatment; July 24–27 2005, Rio de Janeiro, Brazil.

37 Clotet, B.; Bellos, N.; Molina, J.-M.; Cooper, D.; Goffard, J.-C.; Lazzarin, A.; Wohrmann, A.; Katlama, C.; Wilkin, T.; Haubrich, R.; Cohen, C.; Farthing, C.; Jayaweera, D.; Markowitz, M.; Ruane, P.; Spinosa-Guzman, S.; Lefebvre, E. Efficacy and Safety of Darunavir-Ritonavir at Week 48 in Treatment-experienced Patients with HIV-1 Infection in POWER 1 and 2: a Pooled Subgroup Analysis of Data from Two Randomised Trials. *Lancet* **2007**, *369*, 1169–1178.

38 FDA approves Darunavir on June 23, 2006: FDA approved new HIV treament for patients who do not respond to existing drugs. Please see http://www.fda.gov/bbs/topics/NEWS/2006/NEW01395.html

39 Amano, M.; Koh, Y.; Das, D.; Li, J.; Leschenko, S.; Wang, Y.-F.; Boross, P. I.; Weber, I. T.; Ghosh, A. K.; Mitsuya, H. A Novel *Bis*-Tetrahydrofuranylurethane-Containing Nonpeptidic Protease Inhibitor (PI), GRL-98065, Is Potent against Multi-PI-Resistant Human Immunodeficiency Virus *In Vitro*. *Antimicrob. Agents Chemother.* **2007**, *51*, 2143–2155.

40 Spaltenstein, A.; Kazmierski, W. M.; Miller, J. F.; Samano, V. Discovery of Next Generation Inhibitors of HIV Protease. *Curr. Top. Med. Chem.* **2005**, *5*, 1589–1607.

41 Ghosh, A. K.; Sridhar, P. R.; Leshchenko, S.; Hussain, A. K.; Li, J.; Kovalevsky, A. Y.; Walters, D. E.; Wedekind, J. E.; Grum-Tokars, V.; Das, D.; Koh, Y.; Maeda, K.; Gatanaga, H.; Weber, I. T.; Mitsuya, H. Structure-based Design of Novel HIV-1 Protease Inhibitors to Combat Drug Resistance. *J. Med. Chem.* **2006**, *49*, 5252–5261.

42 Miller, J. F.; Andrews, C. W.; Brieger, M.; Furfine, E. S.; Hale, M. R.; Hanlon, M. H.; Hazen, R. J.; Kaldor, I.; McLean, E. W.; Reynolds, D.; Sammond, D. M.; Spaltenstein, A.; Tung, R.; Turner, E. M.; Xu, R. X.; Sherrill, R. G. Ultra-Potent P_1 Modified Arylsulfonamide HIV Protease Inhibitors: The Discovery of GW0385. *Bioorg. Med. Chem. Lett.* **2006**, *16*, 1788–1794.

43 Clemente, J. C.; Moose, R. E.; Hemrajani, R.; Whitford, L. R.; Govindasamy, L.; Reutzel, R.; McKenna, R.; Agbandje-McKenna, M.; Goodenow, M. M.; Dunn, B. M. Comparing the Accumulation of Active- and Nonactive-site Mutations in the HIV-1 Protease. *Biochemistry* **2004**, *43*, 12141–12151.

44 Chen, Z.; Li, Y.; Chen, E.; Hall, D. L.; Darke, P. L.; Culberson, C.; Shafer, J. A.; Kuo, L. C. Crystal Structure at 1.9-Å Resolution of Human Immunodeficiency Virus (HIV) II Protease Complexed with L-735,524, an Orally Bioavailable Inhibitor of the HIV Proteases. *J. Biol. Chem.* **1994**, *269*, 26344–26348.

Hiroaki Mitsuya*,†, Kenji Maeda*, Debananda Das*, and Arun K. Ghosh‡

*The Experimental Retrovirology Section, HIV and AIDS Malignancy Branch, Center for Cancer Research, National Cancer Institute, Bethesda, Maryland 20892

†Department of Hematology and Infectious Diseases, Kumamoto University School of Medicine, Kumamoto 860–8556

‡Departments of Chemistry and Medicinal Chemistry, Purdue University, West Lafayette, Indiana 47907

Development of Protease Inhibitors and the Fight with Drug-Resistant HIV-1 Variants

I. Chapter Overview

The development of antiretroviral therapy for acquired immunodeficiency syndrome (AIDS) has witnessed one of the most dramatic progressions in the history of medicine. By the late 1980s, it had become apparent that combination chemotherapy with two nucleoside reverse transcriptase inhibitors (NRTIs) was more effective than NRTI monotherapy. However, only with the advent of protease inhibitors (PIs) in early 1990s, providing highly active antiretroviral therapy (HAART), significant clinical benefits became to be seen.

Advances in Pharmacology, Volume 56

1054-3589/08 $35.00
DOI: 10.1016/S1054-3589(07)56006-0

In this chapter, we discuss the principle and utility of development of PIs and the present challenges in the fight with emergence of PI-resistant HIV-1 variants.

II. Introduction

One can say that the development of antiretroviral therapy for AIDS has traced one of the most dramatic progressions in the history of medicine, showing combinations of rapid drug development, short-lived trends, and continuous evolution. In the latter half of 1980s, in the United States, efforts had been made to bring synergism to the basic research programs of the US government, private sectors, and academics on *Human immunodeficiency virus 1* (HIV-1), and to translate the basic findings into rapid development of novel therapeutics for AIDS. A focus of research on HIV-1 protease, the virally encoded enzyme has been targeted following the therapeutic success achieved by targeting at HIV-1 reverse transcriptase (Mitsuya and Erickson, 1999). Initially such an entirely new area of research was not financially well supported by industries. Moreover, the clinical utility of PIs, which had been designed using the knowledge of the molecular structure of protease, was not known. However, it had become apparent that combination chemotherapy with two NRTIs, zidovudine (azidothymidine, AZT) (Mitsuya *et al.*, 1985) and didanosine (dideoxyinosine, ddI) (Mitsuya and Broder, 1986; Yarchoan *et al.*, 1989a,b) was more effective than monotherapy as opposed to using the drugs sequentially (Yarchoan *et al.*, 1994). Between December 1995 and March 1996, three PIs, saquinavir (SQV), followed by ritonavir (RTV), and indinavir (IDV), were approved as prescription drugs for therapy of AIDS through the fast track approval mechanism by the US Food and Drug Administration (FDA) (Mitsuya and Erickson, 1999). Combination chemotherapy, with one of the PIs added to the combined NRTIs, produced sensational results in comparison to the clinical data that had been previously reported.

III. Targeting Viral Protease

A. Mechanism of Action of PIs

HIV-1 encodes a protease, also known as a proteolytic enzyme, which is responsible for the posttranslational processing of the viral products and is required for viral infectivity. Indeed, a mutation of the protease active site aspartic acids or chemical inhibition of the enzyme leads to the production of immature, noninfectious viral particles (Ghosh *et al.*, 2006a,b; Mitsuya and Erickson, 1999; Turk, 2006). The HIV-1 protease is an aspartyl protease that cleaves the HIV Gag and Gag-Pol polyproteins to generate structural

proteins and enzymes of the virus. This processing occurs late in the HIV life cycle during assembly and release from the infected cell and is an essential step for the formation of mature virus particles.

The dimeric HIV-1 protease consists of two identical monomer subunits of 99 amino acids and has an active site that lies at the dimer interface with each monomer contributing a single catalytic aspartic acid residue (Asp-25 and Asp-25′) (Fig. 1). The active site of the enzyme is unusual in that it is formed at the dimer interface and contains two conserved catalytic aspartic acid residues, one from each monomer. The substrate-binding cleft that surrounds the active site contains both hydrophobic and hydrophilic elements. Each monomer of the protease has a β-hairpin region (residues 45–56; Fig. 1) that overlaps to form a "flap" that extends over the binding cleft for the substrate. The flap is flexible enough to allow entry and exit of the polypeptide substrates and undergoes large localized conformational changes during the binding and release of inhibitors and substrates. Indeed, Hornak and their colleagues have shown using molecular dynamics simulation techniques that the unliganded HIV-1 protease flaps spontaneously open and reclose and that the flaps of the unliganded protease open to a much greater degree than observed in crystal structures and subsequently

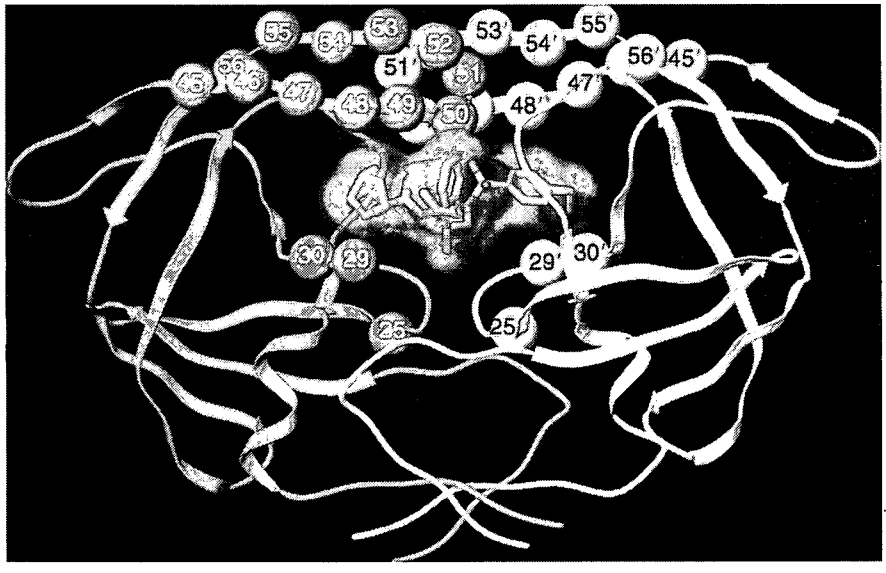

FIGURE 1 Structure of HIV-1 protease. The HIV protease consists of two identical 99 amino acid subunits and has an active site that lies at the dimer interface with each monomer contributing a single catalytic aspartic acid residue (Asp-25 and Asp-25′). Each monomer contributes amino acids (positions 45–56) to form a flap that extends over the substrate-binding cleft. The active site is covered by two β-hairpin structures or "flaps" that are highly flexible and undergo large localized conformational changes during the binding and release of inhibitors and substrates.

return to the semi-open state (Hornak *et al.*, 2006). For each substrate, three to four amino acids located on either side of the peptide bond cleavage site are utilized for binding to the substrate cavity of protease. Protease must cleave the immature HIV-1 polyprotein precursors, Gag and Gag-Pol, in at least nine different cleavage sites for maturation to occur (Jacobsen *et al.*, 1992). There is very little homology in the primary amino acid sequences of each of these cleavage sites. Instead, substrate specificity appears to be dictated by the secondary structure that remains conserved in each of the different cleavage sites.

Knowledge of the structure and functions of viral protease has led to the successful development of a wide variety of potent and chemically diverse inhibitors that have been designed using substrate- and structure-based approaches. The first PIs were designed in the early 1990s; those inhibitors were designed in such a way that the inhibitors fit exactly into the active site of the enzyme (Kempf *et al.*, 1990; Sommadossi, 1999). There are currently nine PIs approved for the treatment of HIV-1 infection (Fig. 2). All are competitive inhibitors that bind to the protease active site.

B. Protease Structures and Substrate-Based Inhibitors

In theory, antiviral drugs exert their effects by interacting with viral structural components, virally encoded enzymes, viral genomes, or specific host proteins such as cellular receptors, enzymes, or other factors required for viral replication (Mitsuya and Broder, 1987; Mitsuya and Erickson, 1999; Mitsuya *et al.*, 1990; Turk, 2006). In principle, any virus-specific steps in the replicative cycle of HIV-1, which differs from that in normal host cell function, can serve as a potential target for the development of antiretroviral therapy.

The close structural and functional relationships between retroviral and cellular aspartic proteases, together with knowledge of the HIV-1 protease cleavage site sequences on polyproteins, immediately opened an avenue of peptidomimetic substrate-based approaches that had been developed for designing inhibitors of human renin, an aspartic protease that has long been an important target for the design of antihypertensive agents. Substrate-based inhibitors are essentially peptide substrate analogues in which the scissile peptide bond has been replaced by a non-cleavable, transition-state analogue or isostere. Examples of this class of inhibitors include the first FDA-approved PI, SQV (Fig. 2), which essentially mimics the Phe-Pro cleavage site sequence (Roberts *et al.*, 1990).

C. Design of Symmetry-Based Inhibitors

With the understanding that HIV-1 protease is a twofold (C2) symmetric homodimer in which the active site is formed at the dimer interface and is

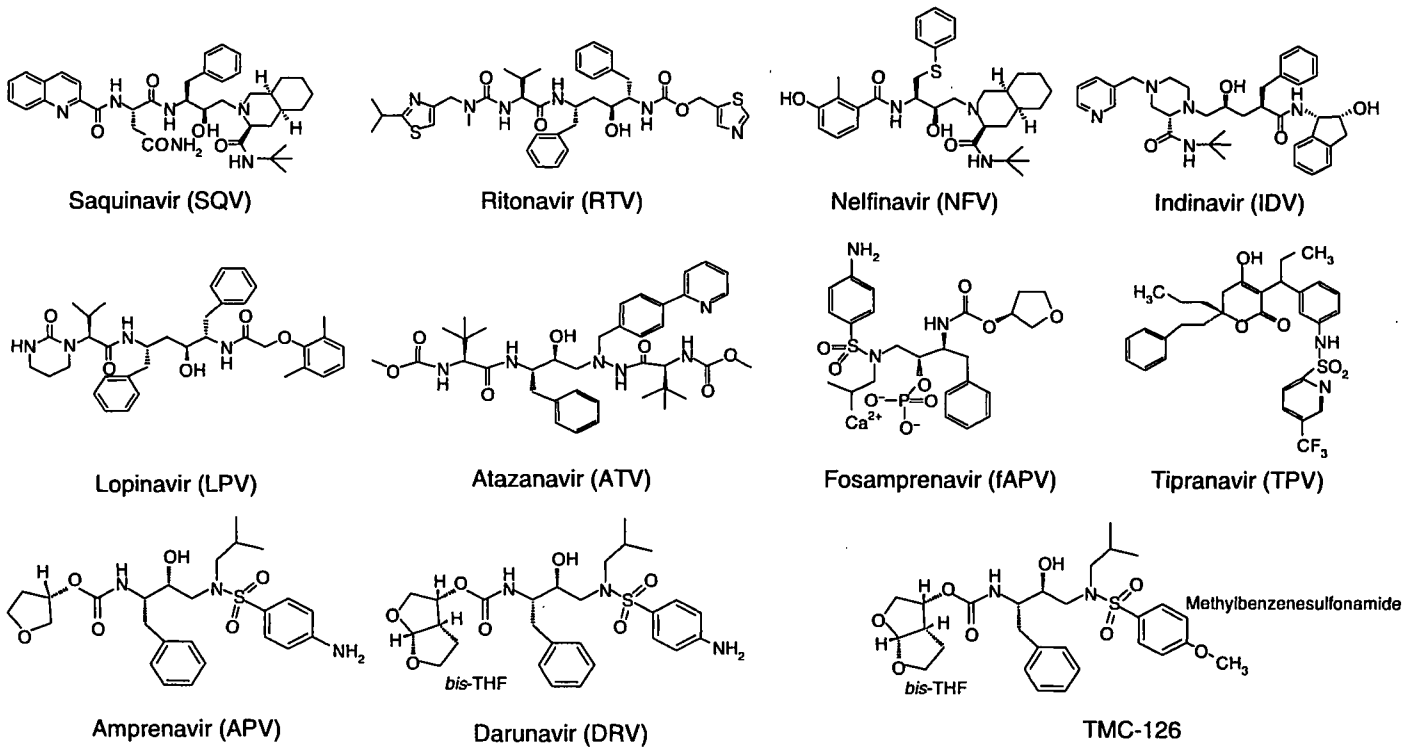

FIGURE 2 Clinically approved PIs. Structures of 10 PIs, thus far FDA-approved, are shown. Fosamprenavir is the prodrug for amprenavir. TMC-126 (not used in humans) is a prototype to darunavir.

composed of equivalent contributions of residues from each subunit came the realization that symmetry could be incorporated into the design of inhibitors for the HIV enzyme. Such designs represented a departure from traditional medicinal chemistry approaches to enzyme inhibitor designs (Erickson *et al.*, 1990; Kempf *et al.*, 1990). Examples for this type of PIs include RTV (Fig. 2).

D. Structure-Based PIs

As of today, well over 200 crystal structures have been solved and deposited in the Protein Data Bank (PDB) for various HIV-1 protease/inhibitor complexes—a testimony to the importance placed on structural information in the process of inhibitor design (Fitzgerald and Springer, 1991; Mitsuya and Erickson, 1999). Combined with medicinal chemistry and, in some cases, target-based screening efforts, these structural investigations have led to a structurally diverse compendium of inhibitors that include inhibitors like nelfinavir (NFV), that were derived solely using structure-based design methods, indinavir (IDV), and amprenavir (APV), the design of which was a blend of medicinal chemistry and structural insights (Fig. 2).

IV. The Role of PIs and Challenges in HAART

HAART, which typically exploits two reverse transcriptase inhibitors (RTIs) and one PI combined (or "boosted," *vide infra*) with RTV, has had a major impact on the AIDS epidemic in industrially advanced nations. However, no eradication of HIV-1 appears to be currently possible, in part, due to the viral reservoirs remaining in blood and infected tissues. Moreover, we have encountered a number of challenges in bringing about the optimal benefits of the currently available therapeutics of AIDS and HIV-1 infection to individuals receiving HAART (De Clercq, 2002; Siliciano *et al.*, 2004; Simon and Ho, 2003). They include (1) drug-related toxicities, (2) partial restoration of immunologic functions once individuals developed AIDS, (3) development of various cancers as a consequence of survival prolongation, (4) flame-up of inflammation in individuals receiving HAART or immune reconstruction syndrome (IRS), and (5) increased cost of antiviral therapy (Carr, 2003; Fumero and Podzamczer, 2003; Grabar *et al.*, 2006; Hirsch *et al.*, 2004; Little *et al.*, 2002).

Unlike the case for the majority of RTIs, most HIV-1 PIs had pharmacokinetic limitations. Poor oral absorption, serum–protein binding, and liver enzyme metabolism can eliminate the antiviral benefits of many otherwise highly potent PIs. PIs need to be ingested often and in large quantities to maintain effective antiviral concentrations in the blood. Furthermore, of the currently available antiviral drugs for HIV-1 infection, PIs are among the most effective, but they are costly and require complicated treatment regimens. Problematic

features of PIs are mostly inherent to their chemical natures: (1) high pill burden, (2) frequent dosing regimens, and (3) various side effects including lipodystrophy and dyslipidemia, although PIs remain an essential component of combination chemotherapy for both drug-naive and treatment-experienced patients with AIDS. It is worth noting that NRTIs are associated with critical adverse effects including mitochondrial toxicity. The role of PIs in HAART has been important and even PI-only regimens have been considered.

As soon as the first PIs were administered in humans, it was found that all PIs are inhibitors of the CYP3A4 system that is the major enzyme catabolizing most PIs and numerous other drugs. It catabolizes more than 50% of marketed drugs and is also frequently involved in drug–drug interactions (Overington *et al.*, 2006). RTV is by far the strongest inhibitor of CYP3A4, and SQV the weakest. Indeed, coadministration of low-dose RTV boosts the exposure of most PIs, which facilitates flexible dosing, including once daily dosing (*vide infra*).

V. "Boosting": A Critical Modification of Clinical Efficacy of PIs

Soon after the development of the first PIs, a problem inherent to this class of inhibitors was recognized, that is, poor pharmacokinetics, low maximum concentration (C_{max}), low plasma trough levels (C_{trough}), and short plasma half-life. The isoenzyme CYP3A4, a subunit of the cytochrome *P450* hepatic enzyme system, is mostly responsible for such poor pharmacokinetic parameters. RTV is by far the most potent inhibitor of the isoenzyme CYP3A4, and it was soon learned that concomitant administration of small doses of RTV with a PI allows "boosting" of the most important phamacokinetic parameters of almost all PIs (Kempf *et al.*, 1997). The unexpected but highly beneficial interactions between RTV and the other PIs have simplified otherwise complex regimens by reducing the frequency and number of pills to be administered, and in many cases by making dosing independent of food intake. Indeed, when boosted, PIs such as fosamprenavir and atazanavir can be taken only once a day. Moreover, boosting of certain PIs such as IDV or APV appears to make such PIs more effective against PI-resistant HIV-1 variants probably by elevating their plasma levels (Condra *et al.*, 2000). However, cautions should be used since plasma levels of PIs may decrease after long durations of treatment. For example, Gisolf *et al.* (2000) have reported that plasma levels of SQV even with RTV boosting dropped by 40% after a 10-month period of therapy. Thus, if there is any suspicion of reduced efficacy of boosted PI treatment after months of therapy, it is recommended that plasma levels of PI be examined and dose adjustments be made.

Until recently, only a limited set of data was available regarding the comparison of the clinical efficacy of each "boosted" PI-containing regimen. However,

there has recently been a wide range of settings where "boosted" PIs are being examined to compare clinical features of each member of PIs with or without other classes of antiretroviral agents. Indeed, the Department of Health and Human Services (DHHS) Guidelines (issued in October, 2006) (DHHS, 2006) recommends that first-line antiretroviral therapy be initiated with either an efavirenz-based regimen or the one containing twice-daily lopinavir/RTV, twice-daily fosamprenavir/RTV, or once-daily atazanavir/RTV. For example, the results of the KLEAN study involving antiretroviral-naive patients with HIV-1 infection have shown that lopinavir/RTV soft-gel capsules (SGC) *bid* and fosamprenavir/RTV *bid* with abacavir/lamivudine fixed dose combination (FDC) performed similarly with regard to virological and immunologic effects as well as adverse effects such as lipid elevations. Moreover, none of the patients with virological failure on either regimen had major PI resistance amino acid substitutions in their HIV-1 (Eron *et al.*, 2006). There are also new data showing that lopinavir/RTV SGC, when used as a once-a-day regimen combined with tenofovir and emtricitabine *qd*, maintains high levels of antiviral activity comparable to the twice-daily regimen in drug-naive patients (Johnson *et al.*, 2006). The results of the RESIST study have shown that tipranavir/RTV delivers better outcomes over comparator "boosted" PIs in highly treatment-experienced patients, although the role of the TPV/RTV combination in salvage therapy is likely to be modest due to its safety, pharmacokinetic issues (twice-daily regimen, etc.), and the near-future increasing availability of other more attractive antiretroviral drugs (Hicks *et al.*, 2006). Taken together, continuing evaluations of "boosted" PI-including regimens should certainly merit to improve the efficacy of HAART.

VI. Viral Resistance to PIs

As described above, HAART has had a major impact on the AIDS epidemic in industrially advanced nations; however, we have also encountered a number of challenges in bringing about the optimal benefits of the currently available therapeutics of AIDS to individuals receiving HAART (De Clercq, 2002; Siliciano *et al.*, 2004; Simon and Ho, 2003). Such limitations and flaws of HAART are worsened by the development of drug-resistant HIV-1 variants (Carr, 2003; Fumero and Podzamczer, 2003; Grabar *et al.*, 2006; Hirsch *et al.*, 2004; Little *et al.*, 2002). Table I illustrates mutations conferring high and intermediate resistance to currently approved PIs.

A. Emergence of Drug Resistance to PIs

A variety of drug resistance mechanisms are at play with PIs. The most important ones from a purely drug-binding standpoint are mutations in the